BIOCHEMISTRY
including biophysical chemistry & molecular biology

Article

pubs.acs.org/biochemistry

Structural Organization of the Nine Spectrin Repeats of Kalirin

K. S. Vishwanatha,[†] Y. P. Wang,[†] H. T. Keutmann,[§] R. E. Mains,[†] and B. A. Eipper*[,†,‡]

[†]Department of Neuroscience and [‡]Department of Molecular, Microbial and Structural Biology, University of Connecticut Health Center, Farmington, Connecticut 06030, United States

[§]Endocrine Unit, Massachusetts General Hospital, Boston, Massachusetts 02115, United States

ABSTRACT: Sequence analysis suggests that *KALRN*, a Rho GDP/GTP exchange factor genetically linked to schizophrenia, could contain as many as nine tandem spectrin repeats (SRs). We expressed and purified fragments of Kalirin containing from one to five putative SRs to determine whether they formed nested structures that could endow Kalirin with the flexible rodlike properties characteristic of spectrin and dystrophin. Far-UV circular dichroism studies indicated that Kalirin contains nine SRs. On the basis of thermal denaturation, sensitivity to chemical denaturants, and the solubility of pairs of repeats, the nine SRs of Kalirin form nested structures. Modeling studies confirmed this conclusion and identified an exposed loop in SR5; consistent with the modeling, this loop was extremely labile to proteolytic cleavage. Analysis of a direpeat fragment (SR4:5) encompassing the region of Kalirin known to interact with NOS2, DISC-1, PAM, and Arf6 identified this as the least stable region. Analytical ultracentrifugation indicated that SR1:3, SR4:6, and SR7:9 were monomers and adopted an extended conformation. Gel filtration suggested that ΔKal7, a natural isoform that includes SR5:9, was monomeric and was not more extended than SR5:9. Similarly, the nine SRs of Kal7, which was also monomeric, were not more extended than SR5:9. The rigidity and flexibility of the nine SRs of Kal7, which separate its essential N-terminal Sec14p domain from its catalytic domain, play an essential role in its contribution to the formation and function of dendritic spines.

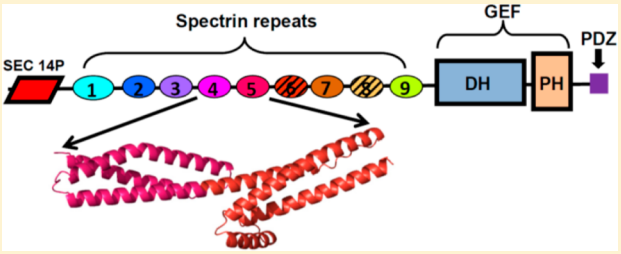

Only four of more than 60 Dbl family Rho GDP/GTP exchange factors (Rho-GEFs) encoded by the human genome include predicted spectrin repeats.[1] The *KALRN* (*ARHGEF24*) and *TRIO* (*ARHGEF23*) genes each encode up to nine spectrin repeats, while the *DBL* (*MCF2*; *ARHGEF21*) and *DBS* (*MCF2L*; *ARHGEF14*) genes include only one spectrin repeat. Neither the function nor the actual structure of these putative spectrin repeats has been examined. In all four proteins, the putative spectrin repeat region separates an N-terminal Sec14p domain from the tandem DH−PH (Dbl homology−pleckstrin homology) domain that catalyzes GDP/GTP exchange. The Sec14p domain of Kalirin binds specific phosphoinositides and is essential for function.[2] Alternative splicing of the *KALRN* gene generates isoforms lacking the Sec14p and first four spectrin repeats, which cannot substitute for full-length isoforms. Kal7, the major full-length isoform of Kalirin in adult brain, is localized at the postsynaptic density (PSD) in the dendritic spines receiving excitatory glutamatergic inputs (Figure 1A). The PH domain of Kal7 interacts with the juxtamembrane region of the NR2B subunit of the NMDA receptor;[3] with its catalytic domain near the plasma membrane, the nine spectrin repeats could position the lipid-binding Sec14p domain of Kal7 outside of the PSD.

Each spectrin repeat consists of a left-handed, antiparallel three-helix bundle 100−120 amino acids in length with aromatic residues at conserved sites; helices A−C are separated by nonhelical linker regions termed the A/B and B/C loops.[4,5] Erythroid and nonerythroid spectrin, with their multiple spectrin repeats and additional interaction domains, provide structural support for the plasma membrane by organizing an extensive cytoskeletal network and binding to multiple soluble and integral membrane proteins.[6] Dystrophin and utrophin, members of the spectrin superfamily, serve similar functions.[7] When expressed in non-neuronal cells, Kal7 is also localized to the subplasma membrane cytoskeleton.[8] On the basis of crystallographic analysis of fragments of spectrin, α-actinin, utrophin, and dystrophin, helix C of one repeat is connected to helix A of the next repeat by a helical linker, forming a functional unit.[7,9−12] The junction between two spectrin repeats forms the ankyrin binding site in β1-spectrin and is sensitive to alterations in orientation.[5,13,14] The putative spectrin repeat region of Kal7 interacts with peptidylglycine α-amidating monooxygenase (PAM), NOS2, DISC-1, HAP1, Arf6, sorting nexins 1 and 2, and αII-spectrin.[15−19] The NOS2 interaction site is the junction between spectrin repeats 4 and 5 (SR4 and SR5, respectively) of Kalirin.[20]

To determine whether the region separating the Sec14p and first GEF domains of Kalirin actually consists of nine spectrin repeats and to manipulate the interaction of Kalirin with its targets, we expressed and purified fragments comprising one to five spectrin repeats. Stable proteins were purified and analyzed using circular dichroism, gel filtration, ultracentrifugation, and

Received: May 4, 2012
Revised: June 23, 2012
Published: June 27, 2012

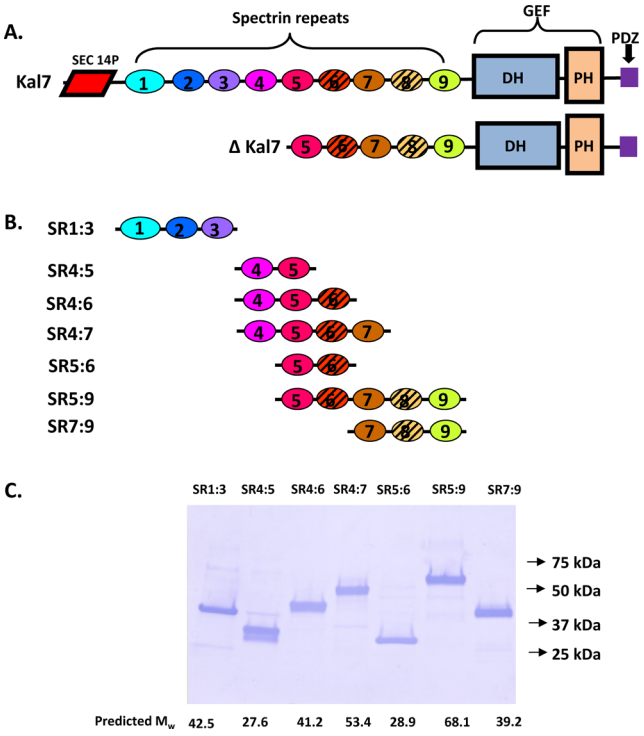

Figure 1. Kalirin proteins examined. (A) Domain structures predicted for Kal7 and ΔKal7, a naturally occurring splice variant. SR6 and SR8, which are not recognized as spectrin-like repeats by SMART, are cross-hatched. The catalytic Dbl homology (DH) domain and adjacent pleckstrin homology (PH) domain form the GDP/GTP exchange factor domain. The C-terminus of Kal7 is a type 1 PDZ binding motif, Ser-Thr-Tyr-Val. (B) The indicated SR proteins were expressed as GST fusion proteins, cleaved, and purified. (C) The seven purified SR proteins studied (1 μg of each) were subjected to SDS−PAGE, transferred to a PVDF membrane, and visualized using Coomassie Brilliant Blue 250. The massess of the molecular weight markers are indicated, as is the molecular weight (M_w) predicted for each SR protein.

molecular modeling. The properties of ΔKal7 and Kal7 were compared to those of the smaller fragments.

MATERIALS AND METHODS

Design and Subcloning of Recombinant Spectrin Repeat Proteins. The numbering scheme for rat Kalirin produced from the a-promoter is used throughout (rat Kalirin-9a, AAF66018.1, GI:7650388). The boundaries of each predicted spectrin repeat were initially defined using the SMART database, which recognizes only seven of the nine domains termed SRs by Alam et al.[15] (http://smart.embl-heidelberg.de); the SR terminology used by Alam et al. is utilized, although neither the region between SR5 and SR7 nor the region between SR7 and SR9 is predicted by SMART to adopt the conformation of a spectrin repeat. To ensure proper folding, we extended the N- and C-termini of the tandem spectrin repeat constructs by a few residues. The start and stop sites for each protein are listed in Table 1; the name of each protein indicates the spectrin repeat regions it includes (e.g., SR4:7 contains spectrin repeats 4−7). cDNAs encoding most of the spectrin repeat fragments were subcloned into the pGEX-6P-2 vector using an upstream *Bam*HI restriction site and a downstream *Not*I site. All vectors were verified by sequencing. A Prescission Protease site separates GST from the spectrin repeat region in the pGEX-6P-2 constructs, while a thrombin site is present in pGEX-4T-2, which was used to produce KalSR4:6.

Table 1. Kalirin Spectrin Repeat (SR) Proteins Expressed[a]

SR fragment	amino acids	M_w	absorption coefficient A_{280}
SR1:3	149−519	42.58	1.029
SR2:4	*282−632*	*40.43*	*insoluble*
SR3:6	*400−870*	*54.45*	*insoluble*
SR3:7	*400−976*	*66.57*	*insoluble*
SR4	517−622	12.26	*insoluble*
SR4:5	517−752	27.16	0.722
SR5	624−752	14.91	*insoluble*
SR5:6	622−870	28.96	0.677
SR4:6	517−873	41.21	0.684
SR4:7	517−976	53.39	0.765
SR7:9	869−1212	39.19	1.270
SR8:9	*966−1219*	*29.72*	*insoluble*
SR5:9	622−1208	68.14	1.108
SR9	1094−1257	19.38	1.106

[a]The boundaries of SR1−5, -7, and -9 were identified using SMART;[15] on the basis of manual alignment, two additional putative SRs were identified (SR6 and SR8). Additional residues were added to the N- and C-termini of the expressed proteins in an attempt to increase their solubility. The name of each protein indicates the first and last putative SR contained in it. The predicted molecular weight (M_w) and absorption coefficient at 280 nm (A_{280}) for a 1.0 mg/mL solution are shown. Each SR fusion protein was well expressed, but several fusion proteins were largely insoluble (shown in italics) and were not further analyzed.

Preparation of Recombinant SR Proteins. The cDNAs encoding each fusion protein were transformed into *Escherichia coli* BL21. To facilitate folding of the recombinant fusion protein, growth and induction [0.4 mM isopropyl β-D-thiogalactopyranoside (Sigma-Aldrich, St. Louis, MO) for 2 h] were conducted at 20 °C; this significantly increased the yield of the soluble product. Yields for each spectrin repeat protein ranged from 0.5 to 5 mg/500 mL of bacterial culture. The cell pellet from a 500 mL culture was washed twice with PBS [50 mM NaP_i and 150 mM NaCl (pH 7.4)], resuspended in 30 mL of PBS, and lysed using a Misonix S4000 ultrasonic liquid processor (Qsonica, LLC, Newtown, CT). Insoluble debris was removed by centrifugation (3 × 14000 rpm for 30 min), and the filtered supernatant was loaded onto a 5 mL GSTrap-4B column (GE Healthcare, Piscataway, NJ) equilibrated with PBS (flow rate of 0.5 mL/min). After equilibration with cleavage buffer [25 mM Tris-HCl (pH 8.0), 150 mM NaCl, and 14 mM β-mercaptoethanol], each SR protein was cleaved from glutathione *S*-transferase using GST-HRVC3 protease (GenWay Biotech, Inc., San Diego, CA) (10 units/mg of fusion protein); the cartridge was incubated with protease overnight at 4 °C. The GST moiety was removed from KalSR4:6 using thrombin (Sigma-Aldrich). Each SR protein was subjected to anion exchange chromatography on a Q-Sepharose column equilibrated with 20 mM NaTES (pH 7.0) and eluted with a gradient to 0.5 M NaCl (60 mL over 120 min) in the same buffer. The purity and homogeneity of each SR protein were evaluated by SDS−PAGE (Bio-Rad Criterion TGX gels, 4 to 15% gradient) followed by staining with Coomassie Brilliant Blue R250. The concentration of each SR protein was determined by measuring its absorbance at 280 nm and using the extinction coefficient calculated from its content of tryptophan and tyrosine (Table 1).

dx.doi.org/10.1021/bi300583s | *Biochemistry* 2012, 51, 5663−5673

Circular Dichroism and Thermal Unfolding. Far-UV CD spectra were recorded using a Jasco J-715 spectropolarimeter equipped with a thermostated cell housing, using a cell with a 1 mm path length. SR proteins (6 μM) were examined between 190 and 260 nm. The molar ellipticity per mean residue, θ in degrees square centimeters per decimole, was calculated from the equation $[\theta] = ([\theta]_{obs}M_{rw})/(10lc)$, where $[\theta]_{obs}$ is the ellipticity measured in degrees, M_{rw} is the mean residue molecular weight (110 g/mol), c is the protein concentration in grams per liter, and l is the optical path length of the cell in centimeters. The scan speed was 10 nm/min at a bandwidth of 1 nm. An average of three runs were recorded for each protein sample. Secondary structure analysis of each SR protein was conducted using CDSSTR[21] with the reference database available in DICHROWEB (http://dichroweb.cryst.bbk.ac.uk/html/home.shtml).

For determination of the thermal unfolding profile, the temperature was increased from 20 to 90 °C at a rate of 1 °C/min and the ellipticity from 190 to 260 nm was recorded at 5 °C intervals. To test for reversibility, all the samples were cooled to 20 °C and the CD spectra were again recorded. Thermal unfolding transitions and midpoints (T_m) were obtained by plotting normalized ellipticity values at 222 nm as a function of temperature.

Unfolding by Chemical Denaturants. Stock solutions of 6 M guanidine hydrochloride and 8 M urea (Sigma-Aldrich) were prepared in 20 mM NaTES (pH 7.0). Concentrations of denaturants were determined by measuring the refractive indices. In each chemical denaturation experiment, recombinant SR protein (final concentration of 2 μM) was incubated for 12 h with either 0−4 M GuHCl or 0−6 M urea at 27 °C in the dark. Unfolding was initiated by addition of a concentrated protein stock to the appropriate denaturant. Unfolding curves were obtained by plotting normalized ellipticity values at 222 nm as a function of denaturant concentration.

Molecular Modeling. For the generation of three-dimensional models of tandem spectrin repeats, we used the automated I-TASSER server (http://zhanglab.ccmb.med.umich.edu/I-TASSER/). Models were displayed and analyzed in PyMOL (DeLano Scientific). To define individual helices along with their connecting loops and to assign individual residues to positions a and d in the heptad hydrophobic repeats, we first aligned the nine spectrin repeat sequences using CLUSTALW (http://www.genome.jp/tools/clustalw/). The boundaries of the helices and connecting loops were then assigned on the basis of the three-dimensional models generated.

Sedimentation Velocity Analysis. Sedimentation velocity experiments were conducted at 20 °C (55000 rpm) in 20 mM NaTES, 200 mM NaCl buffer (pH 7.0) using either interference optics in a Beckman-Coulter XL-I (Brea, CA) analytical ultracentrifuge or fluorescence optics in an XL-I analytical ultracentrifuge equipped with an AU-FDS detector (AVIV). Double-sector cells equipped with quartz windows were used. The rotor was equilibrated under vacuum at 20 °C, and after a period of ∼1 h, the rotor was accelerated to 55000 rpm. Absorbance scans at 280 nm were acquired at ∼4.5 min intervals for 7 h. Protein molecular weights (MW_{seq}), partial specific volumes ($\nu_{20°}$), extinction coefficients (ε_{230}), and buffer density and viscosity were calculated using SEDNTERP.[22] Sedimentation velocity data were analyzed with the time derivative of the concentration profile method using DcDt+ to obtain weight-average sedimentation coefficient distribution $[g(s)]$ values;[23] continuous sedimentation coefficient $[c(s)]$ distribution plots were obtained with SEDPHAT.[23] SEDPHAT analysis yields direct values for the Stokes radius (R_S) and frictional coefficient (f/f_{min}).

Determination of the Stokes Radius by Gel Permeation Chromatography. The Stokes radius was determined using gel filtration chromatography on a Superose 6 10/300 GL column equilibrated with 200 mM NaCl and 20 mM NaTES (pH 7.0). The proteins used for calibration and their Stokes radii were as follows: apoferritin (6.3 nm), human IgG (5.52 nm), bovine serum albumin dimer (4.3 nm), bovine serum albumin monomer (3.55 nm), ovalbumin (2.73 nm), and cytochrome c (1.77 nm).[24] The protein peaks were monitored using a UV detector. For analysis of HisMycKal7 and HisMycΔKal7, pEAK Rapid cells transiently transfected with the appropriate expression vector[2] were lysed in 20 mM NaTES and 10 mM mannitol (pH 7.4); particulate material was removed by centrifugation at 14000g for 15 min, and aliquots of the supernatant were loaded onto the Superose 6 column in the presence of thyroglobulin (1 mg) and bovine serum albumin (1 mg). Aliquots of each fraction were subjected to SDS−PAGE; the elution position was determined after the gels had been stained with Coomassie Brilliant Blue or Western blot analysis using an antibody specific for the C-terminus of Kal7. The void volume (V_0) was determined using high-molecular weight blue dextran. The elution volumes (V_e) of individual standard proteins and SR proteins were recorded. A calibration curve was obtained by plotting the Stokes radius of each standard as a function of elution volume. Because the SRs are elongated, rodlike molecules based on sedimentation analysis, Stokes radii for SR5:9, HisMycKal7, and HisMycΔKal7 were obtained from a calibration curve generated using the R_S values for SRs that were determined by analytical ultracentrifugation. The f/f_{min} values for SR5:9, HisMycKal7, and HisMycΔKal7 were obtained by using the deduced R_S value in Stokes and Perrin equations.[25]

RESULTS

Analysis of Recombinant Kalirin SR Proteins Using Circular Dichroism. Fourteen Kalirin SR proteins containing between one and five putative SRs were expressed as GST fusion proteins (Figure 1 and Table 1). All were expressed at high levels; however, six of the fusion proteins were largely insoluble, and one (SR9) had a very low degree of solubility. The purity of the seven soluble Kalirin SR proteins examined in this study is shown in Figure 1C. The concentration of each purified SR protein was determined using the extinction coefficient calculated from its sequence (Table 1).

The secondary structure of the trirepeat SR1:3 protein was determined by far-UV circular dichroism (CD) spectroscopy (Figure 2A). The intense negative peaks at 208 and 222 nm are typical of proteins with a substantial amount of α-helical structure;[26] analysis with CDSSTR indicates that 58% of the residues in SR1:3 are α-helical (Table 2). The ratio between the minima at 222 and 208 nm was 1.05 for SR1:3, indicating that the helices present in this structure interact with each other.[27] The stability of SR1:3 was assessed by determining its resistance to heat-induced denaturation, which was monitored by CD spectra recorded at 222 nm. Thermal unfolding of SR1:3 could be resolved into two phases (Figure 2B); a steep unfolding curve with a midpoint of 41 °C occurred first, followed by a second transition with a midpoint of 64 °C. The native molar ellipticity was not re-established when the sample

dx.doi.org/10.1021/bi300583s | Biochemistry 2012, 51, 5663−5673

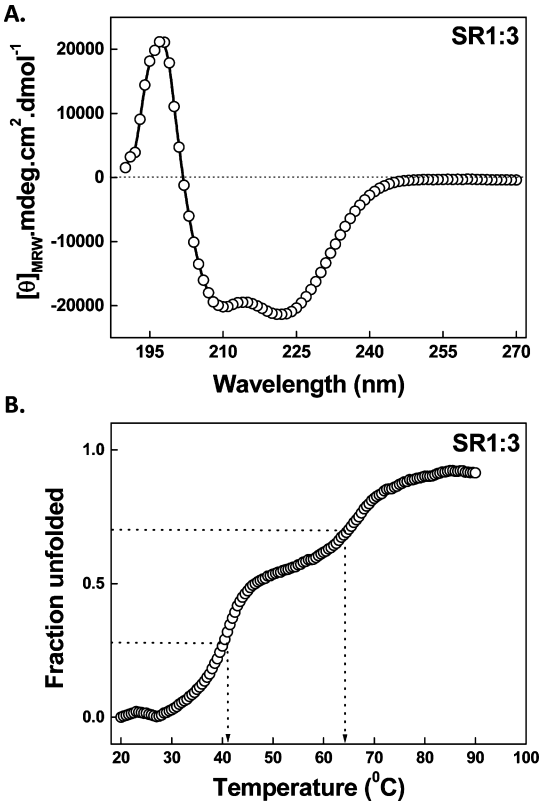

Figure 2. Circular dichroism of SR1:3. (A) Far-UV CD spectrum of SR1:3. (B) Fraction of SR1:3 that was unfolded during a thermal denaturation experiment monitored at 222 nm. Data from multiple analyses of SR1:3 are summarized in Table 2.

Table 2. Evaluation of SR Structure Using Far-UV Circular Dichroism[a]

				T_m (°C)	
SR fragment	% α-helix	θ_{222}	$\theta_{222}/\theta_{208}$	I	II
SR1:3	58	−21526	1.051	41 ± 1.2	64 ± 0.8
SR4:5	58	−23489	1.031	32 ± 1.8	
SR5:6	45	−28564	1.065	42 ± 1.1	
SR4:6	45	−35815	1.090	42 ± 0.3	
SR4:7	47	−25610	1.046	31 ± 0.5	46 ± 1.7
SR7:9	49	−27513	1.058	46 ± 0.9	
SR5:9	42	−23453	1.081	42 ± 1.0	62 ± 2.1
SR9	75	−15380	0.95	33 ± 0.9	

[a]Far-UV CD spectra were obtained for each SR protein. The calculated percentage of the structure identified as α-helix is shown, as is the $\theta_{222}/\theta_{208}$ ratio. Each protein was subjected to thermal denaturation as indicated in Materials and Methods; T_m values represent the average of at least two separate determinations.

was cooled to 20 °C, indicating that the unfolding process was irreversible.

Most of the interactions of Kalirin with other proteins involve spectrin repeats 4−6, making the structure of this region of special interest. In addition, the Δ isoforms of Kalirin lack SR1−4, placing SR5 at the N-terminus. For these reasons, pairs of spectrin repeats were examined (SR4:5 and SR5:6) along with the trirepeat SR4:6 protein that would be present in full-length Kalirin but absent from the Δ Kalirin isoforms (Figure 1A). Far-UV CD spectra for SR4:5, SR5:6, and SR4:6 were typical of proteins rich in α-helical structure (Figure 3A). As observed for SR1:3, the $\theta_{222}/\theta_{208}$ ratios for all three proteins were greater than 1.00 (Table 2). The thermal melting profiles for all three proteins indicated cooperative unfolding with a single T_m. SR4:5 had the lowest thermal stability; a single cooperative transition with a midpoint of 32 °C was observed, suggesting the presence of a poorly ordered domain at physiological temperature (Figure 3B). Although the thermal unfolding profile for SR4:5 shows a "gain of structure" at higher temperatures, the far-UV CD spectra recorded between 190 and 260 nm revealed the presence of unstructured random coils. SR5:6 and SR4:6 were more stable than SR4:5; these proteins each had a T_m of 42 °C, and each unfolded as a single unit (Figure 3B and Table 1). The addition of SR6 to SR4:5 resulted in increased thermal stability, suggesting conformational coupling between spectrin repeats in the central region of Kalirin.

The far-UV CD spectrum of the final trirepeat protein, SR7:9, again revealed a protein with a significant amount of α-helix (49%) and interacting helices (Figure 4A and Table 2). SR7:9 showed a single thermal transition with a midpoint of 46 °C (Figure 4B). To explore the existence of conformational stabilization from adjacent spectrin repeats, we examined two longer SR proteins, SR4:7 and SR5:9. The far-UV CD spectra for both proteins were indicative of structures rich in α-helix with interacting helices (Figure 4A and Table 2). Thermal denaturation of both proteins was biphasic (Figure 4B). Like that of SR4:5, the structure of SR4:7 was unstable at physiological temperature; T_m values of 31 and 46 °C were observed. SR5:9, the entire spectrin repeat region present in the Δ isoforms of Kalirin, exhibited T_m values of 42 and 62 °C (Figure 4B); neither SR5:6 nor SR7:9 had a T_m value as high as that observed for the larger protein.

Chemically Induced Unfolding of Kalirin SR Proteins. To further explore the properties of the spectrin repeat regions critical to the interactions of Kalirin with other proteins, we assessed the ability of SR4:5, SR5:6, SR4:6, and SR4:7 to resist denaturation by guanidine hydrochloride (0−4 M) or urea (0−6 M). Each SR protein was exposed to denaturant for 12 h, and circular dichroism at 222 nm was then assessed (Figure 5 and Table 3). When exposed to either guanidine hydrochloride or urea, SR4:5 unfolded cooperatively, indicating a two-state process (Figure 5); SR4:5 unfolded at a lower concentration of each denaturant than the other SR proteins examined. Complete unfolding of SR5:6 required higher concentrations of both guanidine hydrochloride and urea, with unfolding in guanidine hydrochloride occurring in two stages. The trirepeat SR4:6 and tetrarepeat SR4:7 proteins unfolded in two distinctly different stages, suggestive of regions that unfold independently; both of these larger proteins contained denaturant resistant regions. On the basis of both its lack of thermal stability and its sensitivity to chemical denaturants, SR4:5 is less stable than the surrounding spectrin repeats.

Molecular Modeling of the Spectrin Repeat Region. The biophysical properties of the fragments of Kalirin examined are consistent with the presence of nine spectrin repeats in Kal7. Molecular modeling of each trirepeat protein, SR1:3, SR4:6, and SR7:9, was also consistent with this hypothesis (Figure 6A). When analyzed as part of SR4:6 or SR4:5, the B/C loop of SR5 was predicted to contain a short region of α-helix (Figure 6B). We subjected GST-bound SR4:7 to limited trypsin digestion to determine whether this putative helical region was accessible, as predicted by modeling (Figure 6C). Cleavage products 1−3 were subjected to Edman degradation.

dx.doi.org/10.1021/bi300583s | Biochemistry 2012, 51, 5663−5673

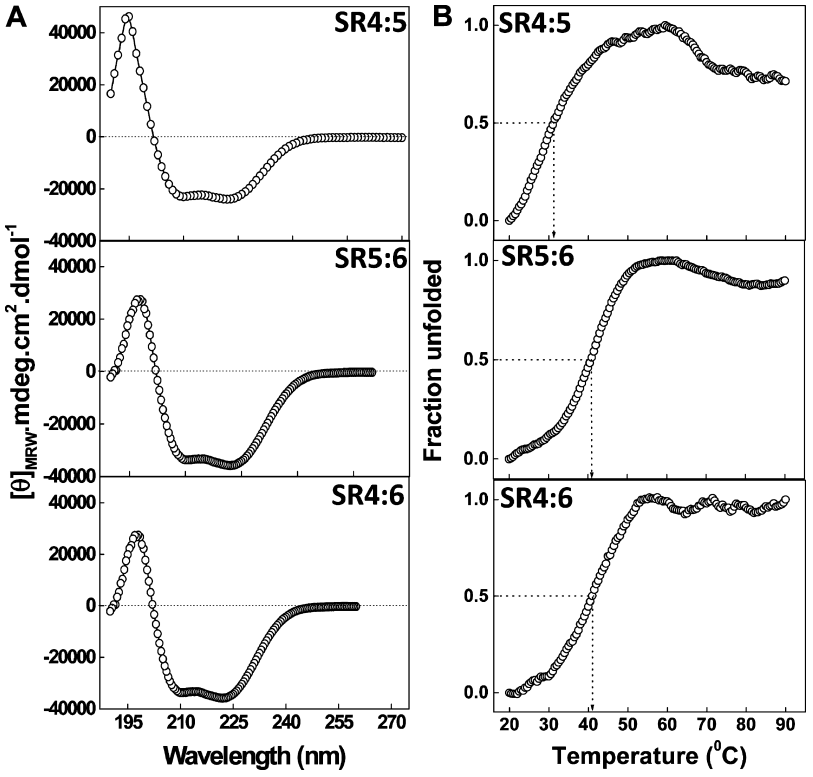

Figure 3. Circular dichroism of SR4:5, SR5:6, and SR4:6. The far-UV CD spectra of SR4:5, SR5:6, and SR4:6 and the fraction of each protein that was unfolded during a thermal denaturation experiment monitored at 222 nm are shown. Data from multiple analyses of SR4:5, SR5:6, and SR4:6 are summarized in Table 2.

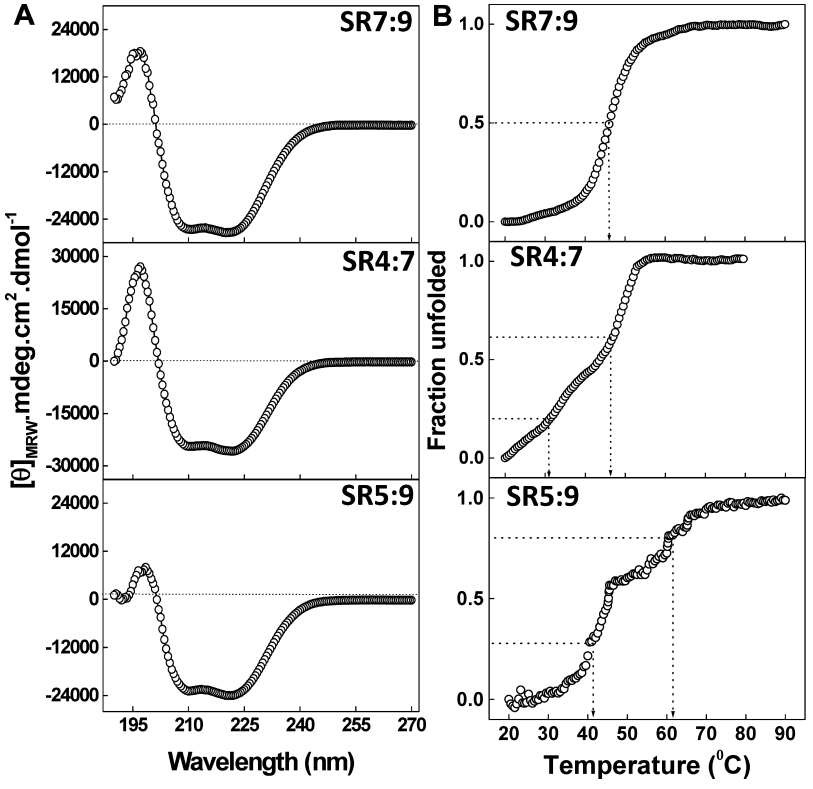

Figure 4. Circular dichroism of SR4:7, SR7:9, and SR5:9. The far-UV CD spectra of SR4:7, SR7:9, and SR5:9 and the fraction of each protein that was unfolded during a thermal denaturation experiment monitored at 222 nm are shown. Data from multiple analyses of SR4:7, SR7:9, and SR5:9 are summarized in Table 2.

dx.doi.org/10.1021/bi300583s | *Biochemistry* 2012, 51, 5663−5673

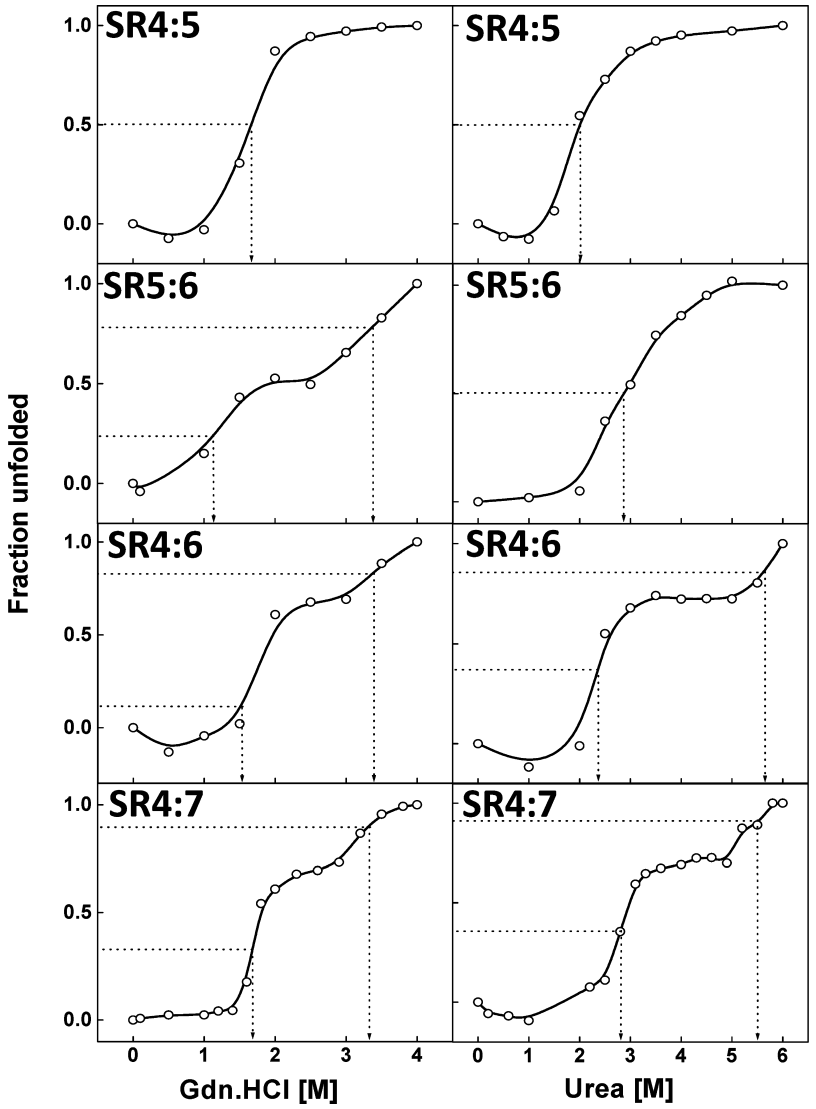

Figure 5. Sensitivity to chemical denaturants. SR4:5, SR5:6, SR4:6, and SR4:7 were incubated in guanidine hydrochloride (0−4.0 M) or urea (0−6.0 M) for 12 h at 27 °C and then subjected to far-UV CD analysis. The fraction of each protein unfolded was assessed by monitoring the signal at 222 nm. Data for the different SR proteins are summarized in Table 3.

Table 3. Guanidine- and Urea-Induced Unfolding of SR Proteins[a]

	$Gdn{\cdot}HCl_{1/2}$ (M)		$urea_{1/2}$ (M)	
SR protein	I	II	I	II
SR4:5	1.66	NA[b]	2.03	NA[b]
SR5:6	1.17	3.37	2.88	NA[b]
SR4:6	1.67	3.36	2.29	5.6
SR4:7	1.67	3.42	2.81	5.48

[a]Data from experiments like those shown in Figure 5 were used to calculate the concentrations of guanidine hydrochloride (Gdn·HCl) and urea producing a half-maximal effect on the structure of each SR protein. [b]Not available.

The first trypsin cleavage separated GST from SR4:7. Sequence data could not be obtained for product 2, suggesting the presence of N-terminal heterogeneity. Product 3, a stable proteolytic product, was generated by cleavage after Arg^{704}, which is located in the short helical region predicted to occur in the B/C loop of SR5.

The sequences of the nine spectrin repeats of Kalirin were aligned on the basis of these structural predictions (Figure 7). The amino acids included in helices A−C and in the A/B and B/C connecting loops were assigned on the basis of the models shown. The amino acids of each heptad repeat are identified as *a*−*g*, with *a* and *d* constituting the hydrophobic core of the coiled coils. The region following the N-terminal Sec14p domain of Kalirin was assigned to SR1; this 142-amino acid region is longer than the typical spectrin repeat. Modeling predicts a long loop preceding helix A of SR1, leaving a short A/B loop connecting helix A to helix B. Seven of the nine SR proteins have tryptophan at position 14 of helix A. The B helix of each spectrin repeat is substantially longer than the A or C helix. The A/B loop of SR8 is substantially longer than other A/B loops and includes a short helical region. The B/C loops of SR1, SR3, SR5, and SR6 range in length from 17 to 21 residues, while the B/C loops of the remaining SRs are much shorter (two to five residues). A binding motif for SH3 domains appears in the B/C loop of SR3 and, as discussed above, a helical region is included in the B/C loop of SR5.

dx.doi.org/10.1021/bi300583s | *Biochemistry* 2012, 51, 5663−5673

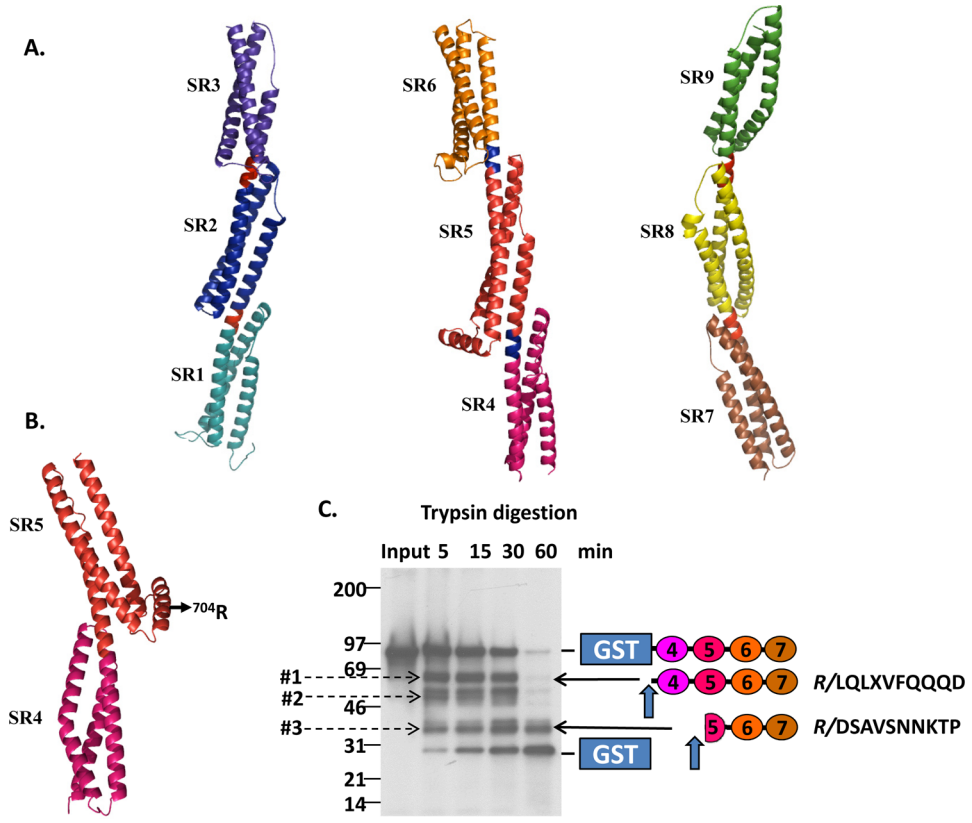

Figure 6. Results of molecular modeling. (A) The sequences of the three trirepeat SR proteins were submitted to the automated I-TASSER server (http://zhanglab.ccmb.med.umich.edu/I-TASSER/). Each SR is indicated by a different color; the linker regions connecting adjacent repeats are colored red (SR1:3 and SR7:9) or blue (SR4:6). (B) The backbone structures predicted for the direpeat SR4:5 protein are shown in an orientation that highlights the helical region in the B/C linker. (C) Purified GST-bound SR4:7 was incubated with immobilized TPCK-trypsin (Pierce) for the times indicated, fractionated by SDS–PAGE, and visualized using antiserum to SR4:7. Only the top and bottom bands were visualized using an antibody to GST; the antiserum used was not affinity-purified and recognizes both SR4:7 and GST. A larger amount of GST-bound SR4:7 was treated with immobilized trypsin for 30 min and fractionated by SDS–PAGE. The Coomassie-stained bands (1–3) indicated by black arrows were excised from the PVDF membrane and subjected to Edman degradation using an Applied Biosystems model 477A pulsed-liquid sequencer with online HPLC identification; the cleavage sites (blue arrows) and sequences obtained are shown.

Hydrodynamic Properties of SR Proteins. Sedimentation velocity analysis was used to determine whether the SR proteins adopted the extended structures predicted by molecular modeling and to determine whether they formed oligomers. Each SR protein was examined at three different concentrations. Analysis of SR1:3, SR4:6, and SR7:9 revealed a single component whose sedimentation velocity was independent of concentration (Figure 8). The evaluation of $S_{20,w}$ from the experimental s value was accomplished by fitting the data to SEDPHAT.[23] Data for each of the SR proteins examined are summarized in Table 4A [apparent molecular weight ($M_{w,app,}$), $S_{20,w}$, and Stokes radius]. The molecular weight of each SR protein measured by sedimentation velocity is very close to the value calculated from the sequence, indicating that each SR protein behaved as a monomer in solution. Reversible self-association was not observed, even at the highest concentration examined (Figure 8); a small amount of aggregated material was present. The experimentally determined Stokes radii indicate that each SR protein adopts an extended rodlike structure, with frictional ratios for the trirepeat proteins varying from 1.46 for SR7:9 to 1.60 for SR1:3.

To compare the properties of the recombinant SR proteins to those of Kal7 and ΔKal7, we utilized gel permeation chromatography. A calibrated Superose 6 column was used to analyze each recombinant protein (Figure 9A). The gel filtration standards analyzed are globular,[25] and a plot of their elution volume versus their Stokes radius generated the expected straight line. Because the SR proteins are rod-shaped, a plot of their elution volumes versus their experimentally determined Stokes radius generated a line shifted to the left (Figure 9A). Gel filtration analysis of purified SR5:9 and cell lysates containing ΔKal7 or Kal7 allowed us to estimate their Stokes radii on the basis of the standard curve generated using purified SR proteins (Figure 9B and Table 4B). Glycerol gradient analysis of ΔKal7 and Kal7 from cell lysates eliminated the possibility that either of these proteins dimerized. The Stokes radius was then used to calculate a frictional ratio (f/f_{min}) for each monomeric protein; SR5:9, with five spectrin repeats, has a frictional ratio greater than that of SR4:7, which has four spectrin repeats. Despite their substantially greater molecular weights, neither ΔKal7 nor Kal7 exhibits greater asymmetry than SR5:9. Kal7, with nine spectrin repeats, has a frictional ratio that is lower than that of ΔKal7.

DISCUSSION

Kalirin Contains Nine Spectrin-like Repeats. Although more variable in length than the SRs of spectrin and dystrophin, our analyses indicate that Kalirin contains nine spectrin repeats. Each SR is ~5 nm long, meaning that a single molecule of Kal7 could extend over 45 nm, a significant distance within the

dx.doi.org/10.1021/bi300583s | Biochemistry 2012, 51, 5663–5673

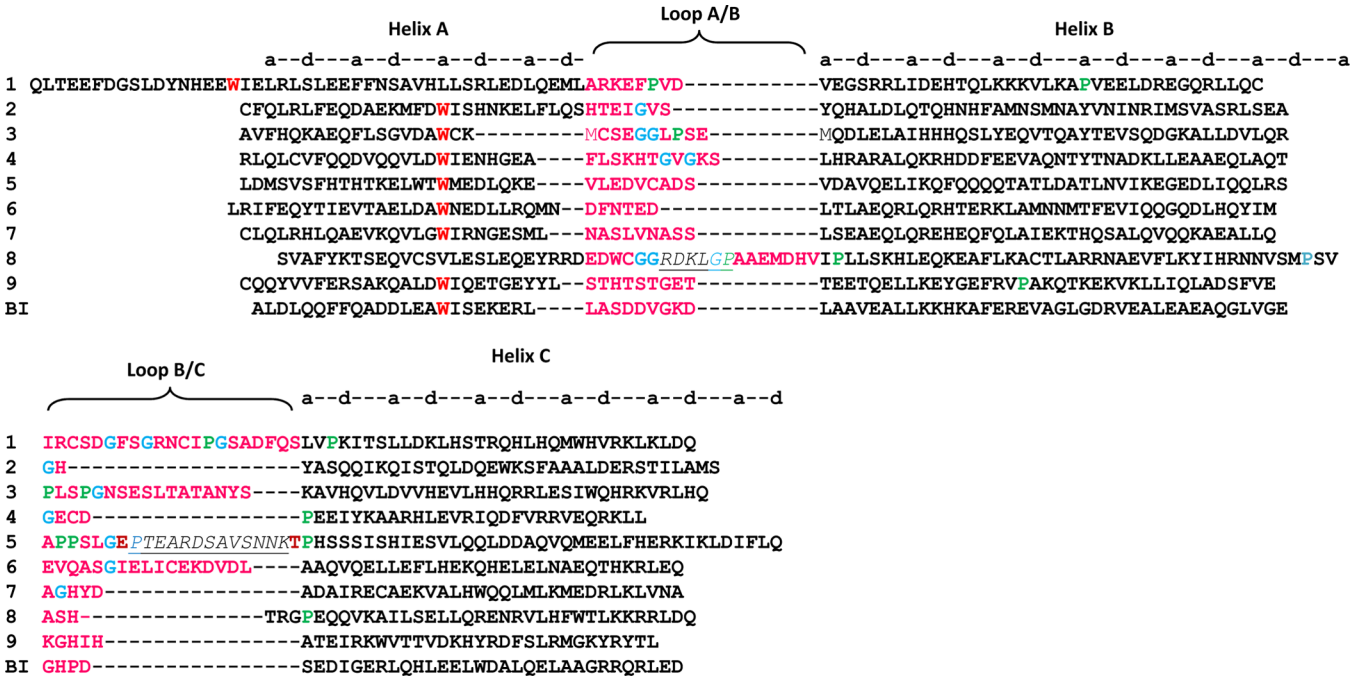

Figure 7. Revised identification of helix and loop regions in the spectrin repeat region of Kalirin. Helices A–C of the nine spectrin repeats of Kalirin identified by molecular modeling are indicated. Pro residues are colored green. Helical regions predicted within the A/B and B/C loops are shown in underlined italics. The sequence of SR1 of human erythroid βI spectrin[5] is shown for comparison.

typical 300 nm diameter and 40 nm thick postsynaptic density.[28] On the basis of circular dichroism, the α-helical content of the Kalirin SRs varied from 42 to 58%; the α-helical content of the 24 spectrin repeats of dystrophin is higher, ranging from 55 to 100%.[29] Conservation of inward-facing nonpolar residues in heptad repeats allows the helices to interact with each other. Our circular dichroism data, with the ratio between the minima at 222 and 208 nm being >1.0 for each Kalirin SR fragment examined, indicate that the helices interact.[27] Thermal denaturation revealed cooperative unfolding of each Kalirin SR fragment, with T_m values between 32 and 64 °C. Direpeat fragments of spectrin exhibited T_m values that varied over the same range (from 36 to 63 °C).[9] The low thermal stability of selected spectrin repeats suggests a role in making the larger protein flexible or in forming a binding site for interacting proteins. While thermal denaturation of individual spectrin repeats is generally reversible, that of tandem repeats is not.[30] None of the Kalirin proteins examined adopted their native conformation after thermal denaturation. The cooperative unfolding of fragments of Kalirin and spectrin required similar concentrations of urea.[9]

Adjacent Spectrin Repeats Form Functional Units. When tandem spectrin repeats are connected by a helical linker that joins helix C of the first unit to helix A of the second unit, an elongated, nonglobular structure is formed and the folding of one spectrin repeat is linked to the folding of neighboring repeats.[9,29,30] SR3 of Kalirin could be stably expressed as part of SR1:3, but not as part of SR3:6 or SR3:7. SR1:3 exhibits two distinct thermal unfolding transitions, suggesting the presence of regions that fold independently. If the presence of SR2 stabilizes SR3, perhaps by joining helix C of SR2 to short helix A of SR3, SR1 may fold separately. On the basis of the analysis of SR4:5, SR5:6, SR4:6, and SR4:7, SR4 is more sensitive to thermal and chemical denaturation than other regions. While SR4:6 exhibits a single thermal unfolding transition, its response to urea and guanidine demonstrates the presence of independent domains. The response of SR5:6 to thermal denaturation and urea suggests the presence of a single unit, leading to the suggestion that SR4 folds separately. Thermal denaturation of SR7:9 occurs with a single transition, indicative of the presence of nested spectrin repeats. The biphasic thermal denaturation of SR5:9 is consistent with the presence of two domains, one formed by SR5:6 and the other by SR7:9. Noncoincidence of thermal and chemical denaturation curves was observed for fragments of human erythroid spectrin,[9] as for SR5:6 and SR4:6; it is difficult to predict which denaturant will reveal the presence of multiple units.

Like SR4:5 of Kalirin, selected repeats in spectrin and dystrophin are largely unfolded at physiological temperature.[9,10] Only the full-length isoforms of Kalirin contain SR4; the Δ-isoforms begin with SR5. The fact that SR4:5 is unfolded at physiological temperatures may provide the conformational flexibility needed for Kalirin to form a docking station for other proteins. The ability of Kalirin to interact with NOS2 was mapped to the 30-amino acid peptide that includes helix C of SR4 and helix A of SR5.[16,20] The binding of PAM,[15] HAP-1,[31] DISC-1,[32] and Arf6[17] to Kalirin has not been as finely mapped but includes this same region. The junction between SR4 and SR5 would be surrounded by the A/B loop of SR4 and the B/C loop of SR5; on the basis of its sensitivity to trypsin, the 13-amino acid α-helical region contained in the B/C loop of SR5 is accessible (Figure 6C). Both desmoplakin[33] and plakin[34] contain spectrin repeats in which a B/C loop contains an additional folded region. Src homology 3 (SH3) domains inserted into the SRs of plakin,[34] desmoplakin,[33] and α-spectrin[35] interact with other proteins. The SH3 binding motif in the B/C loop of SR3 has been shown to interact with the SH3 motif present in the larger isoforms of Kalirin,[36] and the helical folds in the B/C loops of SR5 and SR8 may be engaged in protein–protein interactions.

dx.doi.org/10.1021/bi300583s | *Biochemistry* 2012, 51, 5663–5673

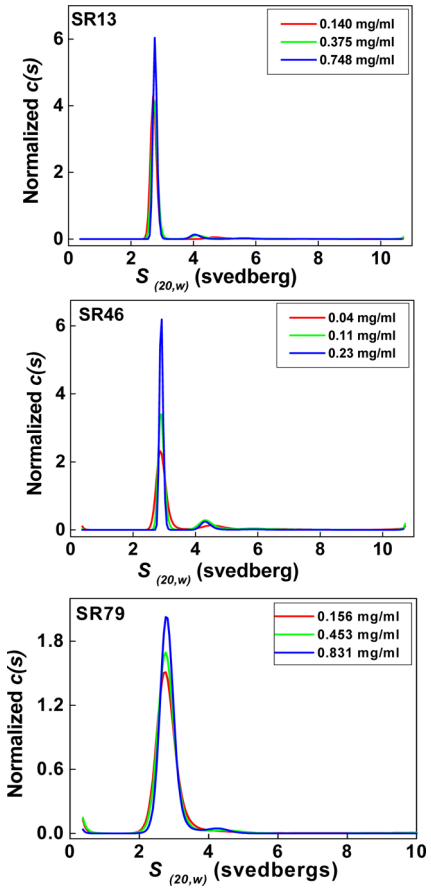

Figure 8. Analytical ultracentrifugation. SR1:3, SR4:5, SR5:6, SR4:6, SR4:7, and SR7:9 were subjected to analytical ultracentrifugation. Data for three concentrations of SR1:3, SR4:6, and SR7:9 are shown; there was no indication of reversible dimerization. The calculated weight for each SR protein analyzed indicates that it is monomeric. The frictional ratios determined (Table 4) indicate that each of these proteins is an extended rod.

Table 4. Evaluation of Hydrodynamic Properties of Kalirin

(A) Sedimentation Velocity Analysis of Kalirin Proteins[a]					
SR protein	M_w (fitted)	ratio to predicted M_w	$S_{20,w}$	R_S (nm)	f/f_{min}
SR1:3	40700	0.956	2.76	3.69	1.60
SR4:5	28400	0.956	2.35	2.76	1.37
SR5:6	30600	1.057	2.32	2.98	1.45
SR4:6	40700	0.988	2.90	3.40	1.47
SR4:7	52100	0.976	3.06	4.14	1.65
SR7:9	42500	1.084	2. 77	3.32	1.46
(B) Gel Filtration Analysis of Kalirin Proteins[b]					
SR protein	M_w (based on sequence)		R_S (nm)		f/f_{min}
SR5:9	68140		4.75		1.75
HisMycΔKal7	119784		5.47		1.71
HisMycKal7	191349		6.13		1.63

[a]Data from analyses like those shown in Figure 8 are summarized. The Stokes radius, R_S, was determined experimentally. R_{min}, the radius of a spherical protein, was calculated from M_w (R_{min} = 0.066 $M^{1/3}$). The frictional ratio, f/f_{min} (=R_S/R_{min}), gives an indication of asymmetry. [b]The proteins analyzed by analytical ultracentrifugation were used to calibrate a Superose 6 column. Recombinant SR5:9, ΔKal7, and Kal7 were analyzed on the same column, and a Stokes radius was assigned on the basis of this calibration curve. Using R_S and R_{min} calculated for a monomer, a frictional ratio was determined.

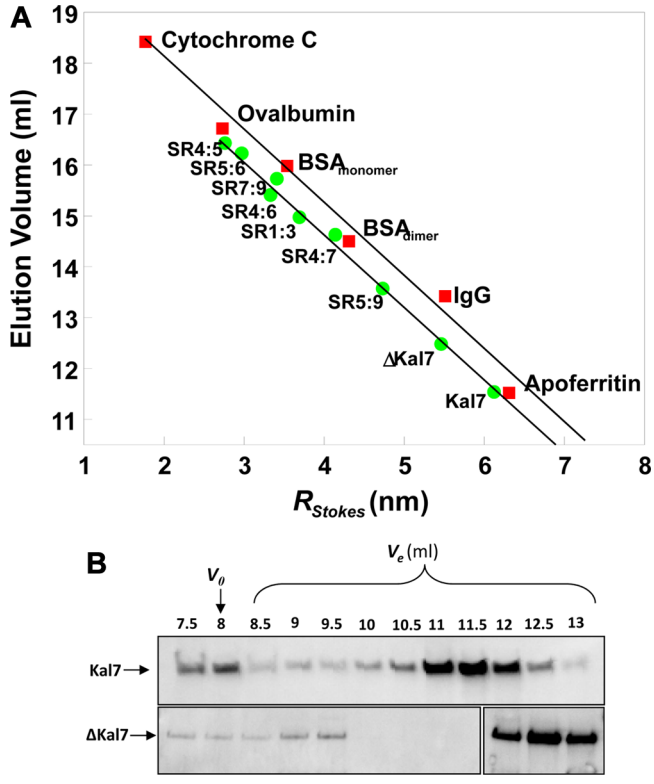

Figure 9. Gel filtration. (A) SR proteins were analyzed on a Superose 6 column calibrated using the indicated globular protein standards. The elution volume for each globular protein is plotted vs its published Stokes radius (red squares).[25] The elution volume for each SR protein subjected to analytical ultracentrifugation is plotted vs its experimentally determined Stokes radius (green circles). (B) Purified SR5:9 and lysates of non-neuronal cells transiently expressing Kal7 or ΔKal7 were analyzed on the same column; their elution volumes were determined by Western blot analysis of individual fractions. On the basis of their experimentally determined elution volumes, Stokes radii were estimated using the best fit line for the SR constructs.

Selected spectrin repeat regions of erythroid and neuronal spectrin[37,38] and dystrophin[39,40] interact with plasma membrane lipids. Preliminary studies suggest that the spectrin repeat regions of Kalirin bind to liposomes; further study will be required to identify the SRs involved and to determine the role of these interactions. As for spectrin and dystrophin, the ability of the spectrin repeat regions of Kalirin to interact with membrane lipids would be expected to play an essential role in its effects on the secretory and endocytic pathways.

High-resolution structures of spectrin repeats from α- and β-spectrin,[11,41−43] α-actinin,[44,45] utrophin,[7,46] and dystrophin[7,12,47] reveal curved helices that wrap around each other. Variability resides in the length and conformation of the A/B and B/C loops and the linkers connecting adjacent repeats. With α-helical linkers connecting adjacent units, the angle between adjacent units can vary substantially. Ankyrin binds tightly to the junction between spectrin repeats 14 and 15 of β-spectrin; because SR15 is tilted compared to SR14, binding is thought to be sensitive to mechanical deformation.[5]

Kalirin Is an Elongated Monomer. The α- and β-chains of spectrin form heterodimers that join in head-to-head tetramers; the helical content and thermal stability of monomeric α- and β-spectrin are similar to those of native spectrin.[48] While α-actinin homodimerizes,[47,49,50] dystrophin is a monomer.[29] On the basis of sedimentation velocity, each of

dx.doi.org/10.1021/bi300583s | Biochemistry 2012, 51, 5663−5673

the Kalirin SR fragments examined is monomeric; while some amount of aggregation was observed, they showed no tendency to form oligomers.

The frictional coefficient, f, depends on the size and shape of the molecule. The f/f_{min} ratio provides a good indication of whether a protein is globular or elongated.[25] Nested SRs form elongated, nonglobular structures,[45] and the f/f_{min} ratios observed for the di-, tri-, and tetra-SR proteins examined (Table 4) indicate that each adopts this type of structure.[49,51−53] SR4:5 and SR5:6 have f/f_{min} ratios of 1.37 and 1.47, respectively. Of the three trirepeat SR proteins examined, SR1:3 has the highest ratio (1.60). The ratio of SR4:7 (1.65) is higher than that of SR4:6 (1.47).

For SR5:9, ΔKal7, and Kal7, f/f_{min} ratios were estimated using a gel filtration column calibrated with the proteins analyzed in the ultracentrifuge; SR5:9 (f/f_{min} = 1.75) appears to be even more extended than SR4:7. The f/f_{min} value of ΔKal7 (1.71) is not increased versus that of SR5:9, indicating that the GEF domain, which crystallographic studies identify as a compact 10 nm × 10 nm × 9.8 nm structure,[54] does not form a rigid extension of SR5:9. The fact that Thr^{1590}, a Cdk5 phosphorylation site located immediately beyond the GEF domain, is readily accessible in constructs that lack any spectrin repeats but is not readily accessible in ΔKal7 is consistent with an intramolecular interaction between the spectrin repeat and C-terminal regions of ΔKal7.[55] Although Kal7 differs from ΔKal7 by the addition of SR1:4 and Sec14p, the f/f_{min} value of Kal7 (1.63) is smaller than that of ΔKal7. Given the instability of SR4, it is tempting to suggest that its presence introduces flexibility into Kal7, allowing its N-terminal region to interact with the rest of the molecule.

AUTHOR INFORMATION

Corresponding Author

*E-mail: eipper@uchc.edu. Phone: (860) 679-8898.

Funding

This work was supported by National Institutes of Health Grant DK-32948 to R.E.M. and by the Janice and Rodney Reynolds Endowment.

Notes

The authors declare no competing financial interest.

ACKNOWLEDGMENTS

We thank Darlene D'Amato for her contributions to all aspects of this work, Li Luo for her assistance with circular dichroism, and Mathilde Bonnemaison for her suggestions about how to present the data. We also thank Dr. Jeffery Lary (Analytical Ultracentrifugation facility, University of Connecticut, Storrs, CT) for his help with the ultracentrifugation study.

ABBREVIATIONS

SR, spectrin repeat; PSD, postsynaptic density; PAM, peptidylglycine α-amidating monooxygenase; GST, glutathione *S*-transferase; CD, circular dichroism; SDS−PAGE, sodium dodecyl sulfate−polyacrylamide gel electrophoresis.

REFERENCES

(1) Rossman, K. L., and Sondek, J. (2005) Larger than Dbl: New structural insights into RhoA activation. *Trends Biochem. Sci. 30*, 163−165.

(2) Schiller, M. R., Blangy, A., Huang, J., Mains, R. E., and Eipper, B. A. (2005) Induction of lamellipodia by Kalirin does not require its guanine nucleotide exchange factor activity. *Exp. Cell Res. 307*, 402−417.

(3) Kiraly, D. D., Lemtiri-Chlieh, F., Levine, E. S., Mains, R. E., and Eipper, B. A. (2011) Kalirin binds the NR2B subunit of the NMDA receptor, altering its synaptic localization and function. *J. Neurosci. 31*, 12554−12565.

(4) Speicher, D. W., and Marchesi, V. T. (1984) Erythrocyte spectrin is comprised of many homologous triple helical segments. *Nature 311*, 177−180.

(5) Stabach, P. R., Simonovic, I., Ranieri, M. A., Aboodi, M. S., Steitz, T. A., Simonovic, M., and Morrow, J. S. (2009) The structure of the ankyrin-binding site of β-spectrin reveals how tandem spectrin-repeats generate unique ligand-binding properties. *Blood 113*, 5377−5384.

(6) Lombardo, C. R., Weed, S. A., Kennedy, S. P., Forget, B. G., and Morrow, J. S. (1994) βII spectrin (fodrin) and βIε 2-spectrin (muscle) contain NH_2- and COOH-terminal membrane association domains (MAD1 and MAD2). *J. Biol. Chem. 269*, 29212−29219.

(7) Winder, S. J., Gibson, T. J., and Kendrick-Jones, J. (1995) Dystrophin and utrophin: The missing links! *FEBS Lett. 369*, 27−33.

(8) Schiller, M. R., Ferraro, F., Wang, Y., Ma, X. M., McPherson, C. E., Sobota, J. A., Schiller, N. I., Mains, R. E., and Eipper, B. A. (2008) Autonomous functions for the Sec14p/spectrin-repeat region of Kalirin. *Exp. Cell Res. 314*, 2674−2691.

(9) MacDonald, R. I., and Cummings, J. A. (2004) Stabilities of folding of clustered, two-repeat fragments of spectrin reveal a potential hinge in the human erythroid spectrin tetramer. *Proc. Natl. Acad. Sci. U.S.A. 101*, 1502−1507.

(10) Kusunoki, H., MacDonald, R. I., and Mondragon, A. (2004) Structural insights into the stability and flexibility of unusual erythroid spectrin repeats. *Structure 12*, 645−656.

(11) Pascual, J., Pfuhl, M., Walther, D., Saraste, M., and Nilges, M. (1997) Solution structure of the spectrin repeat: A left-handed antiparallel triple-helical coiled-coil. *J. Mol. Biol. 273*, 740−751.

(12) Norwood, F. L., Sutherland-Smith, A. J., Keep, N. H., and Kendrick-Jones, J. (2000) The structure of the N-terminal actin-binding domain of human dystrophin and how mutations in this domain may cause Duchenne or Becker muscular dystrophy. *Structure 8*, 481−491.

(13) Davis, L., Abdi, K., Machius, M., Brautigam, C., Tomchick, D. R., Bennett, V., and Michaely, P. (2009) Localization and structure of the ankyrin-binding site on β2-spectrin. *J. Biol. Chem. 284*, 6982−6987.

(14) Ipsaro, J. J., Huang, L., and Mondragon, A. (2009) Structures of the spectrin-ankyrin interaction binding domains. *Blood 113*, 5385−5393.

(15) Alam, M. R., Johnson, R. C., Darlington, D. N., Hand, T. A., Mains, R. E., and Eipper, B. A. (1997) Kalirin, a cytosolic protein with spectrin-like and GDP/GTP exchange factor-like domains that interacts with peptidylglycine α-amidating monooxygenase, an integral membrane peptide-processing enzyme. *J. Biol. Chem. 272*, 12667−12675.

(16) Ratovitski, E. A., Alam, M. R., Quick, R. A., McMillan, A., Bao, C., Kozlovsky, C., Hand, T. A., Johnson, R. C., Mains, R. E., Eipper, B. A., and Lowenstein, C. J. (1999) Kalirin inhibition of inducible nitric-oxide synthase. *J. Biol. Chem. 274*, 993−999.

(17) Koo, T. H., Eipper, B. A., and Donaldson, J. G. (2007) Arf6 recruits the Rac GEF Kalirin to the plasma membrane facilitating Rac activation. *BMC Cell Biol. 8*, 29.

(18) Rabiner, C. A., Mains, R. E., and Eipper, B. A. (2005) Kalirin: A dual Rho guanine nucleotide exchange factor that is so much more than the sum of its many parts. *Neuroscientist 11*, 148−160.

(19) Prosser, D. C., Tran, D., Schooley, A., Wendland, B., and Ngsee, J. K. (2010) A novel, retromer-independent role for sorting nexins 1 and 2 in RhoG-dependent membrane remodeling. *Traffic 11*, 1347−1362.

(20) Youn, H., Ji, I., Ji, H. P., Markesbery, W. R., and Ji, T. H. (2007) Under-expression of Kalirin-7 increases iNOS activity in cultured cells and correlates to elevated iNOS activity in Alzheimer's disease hippocampus. *J. Alzheimer's Dis. 12*, 271−281.

(21) Sreerama, N., and Woody, R. W. (2003) Structural composition of βI- and βII-proteins. *Protein Sci. 12*, 384−388.
(22) Laue, T. M., Shah, B. D., Ridgeway, T. M., and Pelletier, S. L. (1992) Computer-aided interpretation of analytical sedimentation data for proteins. In *Analytical Ultracentrifugation in Biochemistry and Polymer Science* (Harding, S., and Rowe, A., Eds.) pp 90−125, Royal Society of Chemistry, Cambridge, U.K.
(23) Schuck, P. (2003) On the analysis of protein self-association by sedimentation velocity analytical ultracentrifugation. *Anal. Biochem. 320*, 104−124.
(24) Le Maire, M., Arnou, B., Olesen, C., Georgin, D., Ebel, C., and Moller, J. V. (2008) Gel chromatography and analytical ultracentrifugation to determine the extent of detergent binding and aggregation, and Stokes radius of membrane proteins using sarcoplasmic reticulum Ca^{2+}-ATPase as an example. *Nat. Protoc. 3*, 1782−1795.
(25) Erickson, H. P. (2009) Size and shape of protein molecules at the nanometer level determined by sedimentation, gel filtration, and electron microscopy. *Biol. Proced. Online 11*, 32−51.
(26) Sreerama, N., Venyaminov, S. Y., and Woody, R. W. (1999) Estimation of the number of α-helical and β-strand segments in proteins using circular dichroism spectroscopy. *Protein Sci. 8*, 370−380.
(27) Zhang, Y. P., Lewis, R. N., Hodges, R. S., and McElhaney, R. N. (1992) FTIR spectroscopic studies of the conformation and amide hydrogen exchange of a peptide model of the hydrophobic transmembrane α-helices of membrane proteins. *Biochemistry 31*, 11572−11578.
(28) Chen, X., Winters, C., Azzam, R., Li, X., Galbraith, J. A., Leapman, R. D., and Reese, T. S. (2008) Organization of the core structure of the postsynaptic density. *Proc. Natl. Acad. Sci. U.S.A. 105*, 4453−4458.
(29) Mirza, A., Sagathevan, M., Sahni, N., Choi, L., and Menhart, N. (2010) A biophysical map of the dystrophin rod. *Biochim. Biophys. Acta 1804*, 1796−1809.
(30) An, X., Zhang, X., Salomao, M., Guo, X., Yang, Y., Wu, Y., Gratzer, W., Baines, A. J., and Mohandas, N. (2006) Thermal stabilities of brain spectrin and the constituent repeats of subunits. *Biochemistry 45*, 13670−13676.
(31) Colomer, V., Engelender, S., Sharp, A. H., Duan, K., Cooper, J. K., Lanahan, A., Lyford, G., Worley, P., and Ross, C. A. (1997) Huntingtin-associated protein 1 (HAP1) binds to a Trio-like polypeptide, with a rac1 guanine nucleotide exchange factor domain. *Hum. Mol. Genet. 6*, 1519−1525.
(32) Hayashi-Takagi, A., Takaki, M., Graziane, N., Seshadri, S., Murdoch, H., Dunlop, A. J., Makino, Y., Seshadri, A. J., Ishizuka, K., Srivastava, D. P., Xie, Z., Baraban, J. M., Houslay, M. D., Tomoda, T., Brandon, N. J., Kamiya, A., Yan, Z., Penzes, P., and Sawa, A. (2010) Disrupted-in-Schizophrenia 1 (DISC1) regulates spines of the glutamate synapse via Rac1. *Nat. Neurosci. 13*, 327−332.
(33) Choi, H. J., and Weis, W. I. (2011) Crystal structure of a rigid four-spectrin-repeat fragment of the human desmoplakin plakin domain. *J. Mol. Biol. 409*, 800−812.
(34) Ortega, E., Buey, R. M., Sonnenberg, A., and de Pereda, J. M. (2011) The structure of the plakin domain of plectin reveals a non-canonical SH3 domain interacting with its fourth spectrin repeat. *J. Biol. Chem. 286*, 12429−12438.
(35) Bialkowska, K., Saido, T. C., and Fox, J. E. (2005) SH3 domain of spectrin participates in the activation of Rac in specialized calpain-induced integrin signaling complexes. *J. Cell Sci. 118*, 381−395.
(36) Schiller, M. R., Chakrabarti, K., King, G. F., Schiller, N. I., Eipper, B. A., and Maciejewski, M. W. (2006) Regulation of RhoGEF activity by intramolecular and intermolecular SH3 domain interactions. *J. Biol. Chem. 281*, 18774−18786.
(37) An, X., Guo, X., Gratzer, W., and Mohandas, N. (2005) Phospholipid binding by proteins of the spectrin family: A comparative study. *Biochem. Biophys. Res. Commun. 327*, 794−800.
(38) Ray, S., and Chakrabarti, A. (2004) Membrane interaction of erythroid spectrin: Surface-density-dependent high-affinity binding to phosphatidylethanolamine. *Mol. Membr. Biol. 21*, 93−100.
(39) Sarkis, J., Hubert, J. F., Legrand, B., Robert, E., Cheron, A., Jardin, J., Hitti, E., Le Rumeur, E., and Vie, V. (2011) Spectrin-like repeats 11−15 of human dystrophin show adaptations to a lipidic environment. *J. Biol. Chem. 286*, 30481−30491.
(40) Legardinier, S., Raguenes-Nicol, C., Tascon, C., Rocher, C., Hardy, S., Hubert, J. F., and Le Rumeur, E. (2009) Mapping of the lipid-binding and stability properties of the central rod domain of human dystrophin. *J. Mol. Biol. 389*, 546−558.
(41) Yan, Y., Winograd, E., Viel, A., Cronin, T., Harrison, S. C., and Branton, D. (1993) Crystal structure of the repetitive segments of spectrin. *Science 262*, 2027−2030.
(42) Grum, V. L., Li, D., MacDonald, R. I., and Mondragon, A. (1999) Structures of two repeats of spectrin suggest models of flexibility. *Cell 98*, 523−535.
(43) Kusunoki, H., Minasov, G., MacDonald, R. I., and Mondragon, A. (2004) Independent movement, dimerization and stability of tandem repeats of chicken brain α-spectrin. *J. Mol. Biol. 344*, 495−511.
(44) Tang, J., Taylor, D. W., and Taylor, K. A. (2001) The three-dimensional structure of α-actinin obtained by cryoelectron microscopy suggests a model for Ca^{2+}-dependent actin binding. *J. Mol. Biol. 310*, 845−858.
(45) Djinovic-Carugo, K., Gautel, M., Ylanne, J., and Young, P. (2002) The spectrin repeat: A structural platform for cytoskeletal protein assemblies. *FEBS Lett. 513*, 119−123.
(46) Keep, N. H., Winder, S. J., Moores, C. A., Walke, S., Norwood, F. L., and Kendrick-Jones, J. (1999) Crystal structure of the actin-binding region of utrophin reveals a head-to-tail dimer. *Structure 7*, 1539−1546.
(47) Kahana, E., and Gratzer, W. B. (1995) Minimum folding unit of dystrophin rod domain. *Biochemistry 34*, 8110−8114.
(48) Fujita, T., Ralston, G. B., and Morris, M. B. (1998) Purification of erythrocyte spectrin α- and β-subunits at alkaline pH and structural and hydrodynamic properties of the isolated subunits. *Biochemistry 37*, 272−280.
(49) Flood, G., Rowe, A. J., Critchley, D. R., and Gratzer, W. B. (1997) Further analysis of the role of spectrin repeat motifs in α-actinin dimer formation. *Eur. Biophys. J. 25*, 431−435.
(50) Flood, G., Kahana, E., Gilmore, A. P., Rowe, A. J., Gratzer, W. B., and Critchley, D. R. (1995) Association of structural repeats in the α-actinin rod domain. Alignment of inter-subunit interactions. *J. Mol. Biol. 252*, 227−234.
(51) Ralston, G. B. (1978) Physical-chemical studies of spectrin. *J. Supramol. Struct. 8*, 361−373.
(52) Long, F., McElheny, D., Jiang, S., Park, S., Caffrey, M. S., and Fung, L. W. (2007) Conformational change of erythroid α-spectrin at the tetramerization site upon binding β-spectrin. *Protein Sci. 16*, 2519−2530.
(53) Rybakova, I. N., Humston, J. L., Sonnemann, K. J., and Ervasti, J. M. (2006) Dystrophin and utrophin bind actin through distinct modes of contact. *J. Biol. Chem. 281*, 9996−10001.
(54) Skowronek, K. R., Guo, F., Zheng, Y., and Nassar, N. (2004) The C-terminal basic tail of RhoG assists the guanine nucleotide exchange factor trio in binding to phospholipids. *J. Biol. Chem. 279*, 37895−37907.
(55) Xin, X., Wang, Y., Ma, X. M., Rompolas, P., Keutmann, H. T., Mains, R. E., and Eipper, B. A. (2008) Regulation of Kalirin by Cdk5. *J. Cell Sci. 121*, 2601−2611.

NOTE ADDED AFTER ASAP PUBLICATION

This manuscript was published on July 6, 2012. Amino acid values in Table 1 were revised and the corrected version was reposted on July 17, 2012.